

Cathodoluminescence and TEM investigations of structural and optical properties of AlGa_xN on epitaxial laterally overgrown AlN/sapphire templates

U Zeimer¹, A Mogilatenko^{1,2}, V Kueller¹, A Knauer¹ and M Weyers¹

¹Ferdinand-Braun-Institut, Leibniz-Institut für Höchstfrequenztechnik, Gustav-Kirchhoff-Str. 4, 12489 Berlin, Germany

²Humboldt-Universität zu Berlin, Newtonstr. 15, 12489 Berlin, Germany

ute.zeimer@fbh-berlin.de

Abstract. Surface steps as high as 15 nm on up to 10 μm thick AlN layers grown on patterned AlN/sapphire templates play a major role for the structural and optical properties of Al_xGa_{1-x}N layers with $x \geq 0.5$ grown subsequently by metalorganic vapour phase epitaxy. The higher the Ga content in these layers is, the stronger is the influence of the surface morphology on their properties. For $x = 0.5$ not only periodic inhomogeneities in the Al content due to growth of Ga-rich facets are observed by cathodoluminescence, but these facets give rise to additional dislocation formation as discovered by annular dark-field scanning transmission electron microscopy. For Al_xGa_{1-x}N layers with $x = 0.8$ the difference in Al content between facets and surrounding material is much smaller. Therefore, the threading dislocation density (TDD) is only defined by the TDD in the underlying epitaxially laterally overgrown (ELO) AlN layer. This way high quality Al_{0.8}Ga_{0.2}N with a thickness up to 1.5 μm and a TDD $\leq 5 \times 10^8 \text{ cm}^{-2}$ was obtained.

1. Introduction

Light emitting diodes (LEDs) with wavelengths in the ultraviolet (UV)-B and -C regions have the potential to replace UV lamps used for water purification, photo-chemical curing and many other applications due to their higher efficiency and longer lifetime. For effective light extraction through the sapphire substrate Al_xGa_{1-x}N buffer layers with Al content ranging from 0.5 to 0.8 are required which are transparent to the UV light emitted from the active regions of such LEDs. However, when Al_xGa_{1-x}N layers are grown on planar AlN/sapphire templates they have usually a threading dislocation density (TDD) in the range of $> 10^{10} \text{ cm}^{-2}$. This very high TDD reduces the LED efficiency due to nonradiative recombination at dislocations. Therefore several groups developed different approaches to reduce the TDD [1 - 3].

We use lateral epitaxial overgrowth (ELO) over a stripe patterned AlN/sapphire template by metalorganic vapour phase epitaxy (MOVPE) for the reduction of the TDD. First, a thick ELO AlN layer is grown to reach coalescence and a smooth surface which is subsequently overgrown with Al_xGa_{1-x}N. In an earlier paper we studied the influence of substrate miscut and etch depth into the AlN/sapphire template on the TDD and the surface morphology of the ELO AlN. We found that the latter plays the key role for the homogeneity of the subsequently grown Al_xGa_{1-x}N layers [4].

In this paper we concentrate on the interplay of the optical properties of Al_xGa_{1-x}N layers studied using 80 K cathodoluminescence (CL) and their defect structure studied by annular dark-field scanning transmission electron microscopy (ADF-STEM), both in cross-sectional geometry.



2. Experimental

500 nm thick AlN layers were grown at 1400°C on c-plane sapphire substrates by MOVPE. A stripe pattern running parallel to the [1-100]AlN direction with 1.5 μm wide grooves and a pitch of 3 μm was processed using plasma etching. Then, 7 to 10 μm thick AlN layers were grown on the patterned AlN/sapphire template at 1400°C to obtain coalescence as well as smooth and defect reduced AlN. This thick ELO AlN layer was overgrown by a 25 nm thick AlN layer followed by a 1 - 3 μm thick $\text{Al}_x\text{Ga}_{1-x}\text{N}$ layer, both deposited at 1250°C. The Al content in the $\text{Al}_x\text{Ga}_{1-x}\text{N}$ layer was varied between $x = 0.5$ and $x = 0.8$. For the investigation of the structural and optical properties of this layer we used atomic force microscopy (AFM), high resolution X-ray diffraction (HRXRD), CL at 80K using a Gatan Mono-CL4 system on a Zeiss Ultra+ field emission scanning electron microscope (SEM) and ADF-STEM using a JEOL 2200FS transmission electron microscope.

3. Results and discussion

In our earlier paper [4] we have shown that the surface morphology of ELO AlN strongly depends on the miscut direction of the sapphire substrate. A miscut of only 0.25° towards the *m*-direction of the sapphire substrate leads to an ELO AlN surface with 15 nm high periodic steps and a pitch of 3 μm . Such high steps have also been observed by other groups [5]. In contrast, a miscut of 0.25° towards the *a*-direction together with a reduced etching depth leads to a very smooth ELO AlN surface without any steps. On the other hand, the TDD in ELO AlN is not affected by the miscut direction of the template and can be reduced from $> 2 \times 10^{10} \text{cm}^{-2}$ to below $8 \times 10^8 \text{cm}^{-2}$ [6]. The TDD reduction occurs initially due to bending of dislocation lines to the free surface of the AlN wings as well as further dislocation annihilation during the growth of thick layers. This low TDD is the starting point for the growth of the $\text{Al}_x\text{Ga}_{1-x}\text{N}$ buffer layers.

3.1. $\text{Al}_x\text{Ga}_{1-x}\text{N}$ with $x = 0.5$

Using our MOVPE conditions, 3.5 μm thick $\text{Al}_{0.5}\text{Ga}_{0.5}\text{N}$ layers with a smooth surface morphology could be grown only on an underlying ELO AlN layer exhibiting surface steps, whereas on atomically flat ELO AlN 3D nucleation occurred leading to a very rough surface. The $\text{Al}_{0.5}\text{Ga}_{0.5}\text{N}$ layer grown on the stepped ELO AlN showed no cracks despite its high layer thickness. HRXRD reciprocal space maps of 002 and 105 reflections showed this layer to be fully relaxed. In fig. 1, a cross-sectional backscattered electron (BSE) image is shown together with monochromatic 80K CL images obtained at two peaks at 271 nm and 284 nm observed in the CL sum spectrum from the same sample area. The intensity distribution in the two CL images (fig. 1b, c) is strongly anticorrelated. We attribute this behaviour to a periodic change in the Al content x of the $\text{Al}_x\text{Ga}_{1-x}\text{N}$ layer. This compositional inhomogeneity can be explained by faceted $\text{Al}_x\text{Ga}_{1-x}\text{N}$ growth starting at the surface steps of the ELO AlN with a much higher Ga content on the side facets. A detailed explanation for this behaviour can be found elsewhere [4]. From the corresponding wavelengths the Al content was calculated to be $x = 0.45$ on the facets and $x = 0.54$ in the surrounding material.

The consequences of this rather large difference in composition for the defect evolution have been studied in cross-section by ADF-STEM. Fig. 2 shows the distribution of TDs across the interface between the thick ELO AlN, grown at 1400°C, the thin AlN layer grown at 1250°C (called in the following text “LT-AlN”) and $\text{Al}_x\text{Ga}_{1-x}\text{N}$ with a nominal x -value of 0.5 also grown at 1250°C.

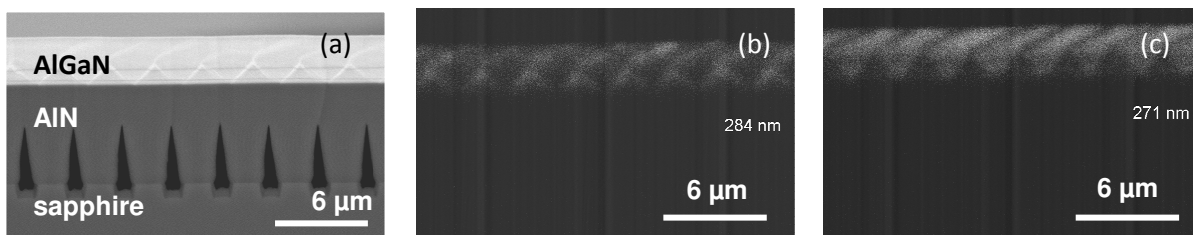


Fig. 1 Cross-section image of a 3.5 μm thick $\text{Al}_{0.5}\text{Ga}_{0.5}\text{N}$ layer grown on ELO AlN: (a) BSE image, (b) and (c) monochromatic 80 K CL images

Besides TDs originating from ELO AlN and penetrating through the ELO AlN/LT-AlN interface into the $\text{Al}_{0.5}\text{Ga}_{0.5}\text{N}$ layer, some dislocations in the ELO AlN are observed that bend near the ELO

AlN/LT-AlN interface and propagate parallel to the interface within the ELO AlN. Also, at the LT-AlN/ $\text{Al}_{0.5}\text{Ga}_{0.5}\text{N}$ interface new dislocations are created. This was expected taking into account the full relaxation of the $\text{Al}_{0.5}\text{Ga}_{0.5}\text{N}$ layer on ELO AlN. One of the steps on the ELO-AlN surface is also seen. Coalescence of the Ga-rich region growing on the side facet of the surface step with the surrounding $\text{Al}_{0.54}\text{Ga}_{0.46}\text{N}$ growing on the planar surface results in formation of an inclined grain boundary. This grain boundary gives rise to dislocations with their line directions inclined with respect to the “normal” TDs. Some of those dislocations annihilate with TDs during proceeding growth. From the half width of rocking curves measured at the 002 and 302 reflections of the $\text{Al}_{0.5}\text{Ga}_{0.5}\text{N}$ layer a TDD of about $4 \times 10^9 \text{ cm}^{-2}$ is estimated. This value is by a factor of 5 higher than the TDD observed in the ELO AlN. In an $\text{Al}_{0.5}\text{Ga}_{0.5}\text{N}$ layer grown in the same run on a planar AlN/sapphire template the TDD is in the range of $3 \times 10^{10} \text{ cm}^{-2}$. Therefore, the growth of $\text{Al}_{0.5}\text{Ga}_{0.5}\text{N}$ on ELO AlN results in a lower defect density as well as in a higher CL intensity (not shown here) compared to growth on planar substrates. Nevertheless, the inhomogeneity of the Al-concentration should be taken into account when using it as a buffer layer material for LEDs.

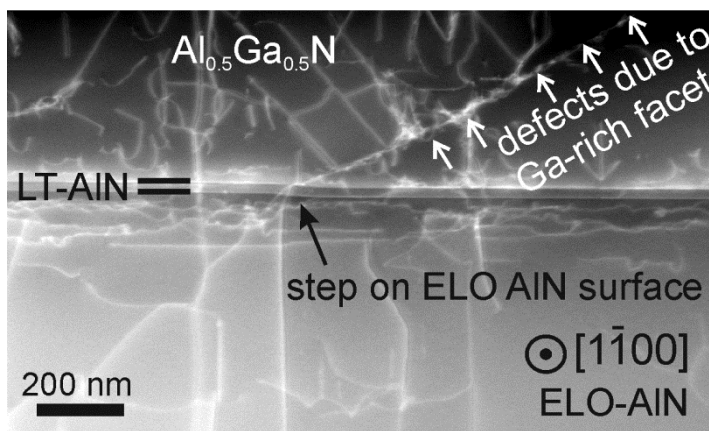


Fig. 2 Cross-sectional ADF-STEM image of the ELO AlN/LT-AlN/ $\text{Al}_{0.5}\text{Ga}_{0.5}\text{N}$ interface region (black arrow points to a step on the ELO AlN surface)

3.2 $\text{Al}_x\text{Ga}_{1-x}\text{N}$ with $x = 0.8$

For LEDs emitting in the UV-C region around a wavelength of 240 nm a higher Al content in the $\text{Al}_x\text{Ga}_{1-x}\text{N}$ buffer layer, i.e. $x = 0.8$, is required. For this purpose an about $1 \mu\text{m}$ thick $\text{Al}_{0.8}\text{Ga}_{0.2}\text{N}$ layer was grown on ELO AlN with surface steps. In the CL spectrum of the cross-section area shown in fig. 3 only one peak has been observed. On the other hand, periodic inhomogeneities in Al content are still observed in the BSE image as well as in the monochromatic CL images. Due to the low Ga content only one Ga-rich facet develops at each step on the ELO AlN surface. From a Gaussian deconvolution of the CL peak using two wavelengths the difference in the Al content between the facets and the surrounding material has been estimated to be no larger than $\Delta x = 0.04$. HRXRD reciprocal space maps of the 002 and 105 reflections revealed a small relaxation below 5%, but ADF-STEM imaging did not show any formation of additional dislocations in the $\text{Al}_{0.8}\text{Ga}_{0.2}\text{N}$ layer (fig. 4).

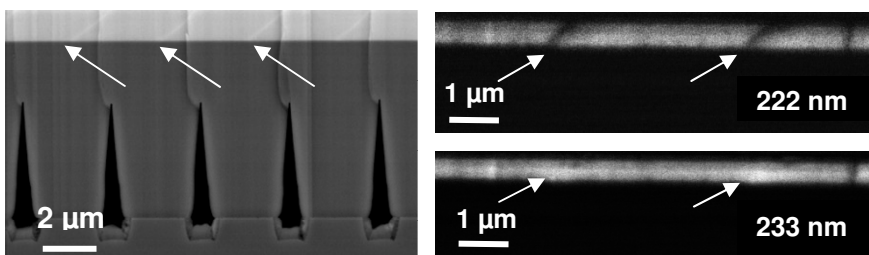


Fig. 3 Cross-section of an $\text{Al}_{0.8}\text{Ga}_{0.2}\text{N}$ layer: (a) BSE-image, (b), (c) 80 K CL images, arrows point to surface steps

However, we observe a certain TD line inclination in $\text{Al}_{0.8}\text{Ga}_{0.2}\text{N}$ whereas TDs in ELO AlN exhibit vertical dislocation lines. Under propagation into the LT-AlN and $\text{Al}_{0.8}\text{Ga}_{0.2}\text{N}$ layers the dislocation line direction changes. Notice that in fig. 4 (obtained in the $[1-100]\text{AlN}$ zone axis) some TD lines seem to maintain their vertical directions. However, our tilting experiments proved that this is a projection effect and that all TDs are inclined toward the $\langle 1-100 \rangle \text{AlN}$ directions. It has been shown

previously that dislocation line inclination in $\text{Al}_x\text{Ga}_{1-x}\text{N}$ layers grown on planar AlN provides relaxation of compressive strain, since the projected length of an inclined dislocation acts as a misfit dislocation segment [7]. In particular, for $\text{Al}_{0.8}\text{Ga}_{0.2}\text{N}$ layers average projected inclination angles in the range of 6° to 10° were observed. Interestingly, here we observe a much higher projected inclination angle of about 20° in $\text{Al}_{0.8}\text{Ga}_{0.2}\text{N}$ on ELO AlN corresponding to a real inclination angle of 30° . Compared to the $\text{Al}_{0.8}\text{Ga}_{0.2}\text{N}$ growth on planar AlN/sapphire the distinct difference is the lower TDD in ELO AlN. Consequently, to achieve compressive strain relaxation a larger TD line inclination resulting in a longer projected length of TD lines would be required.

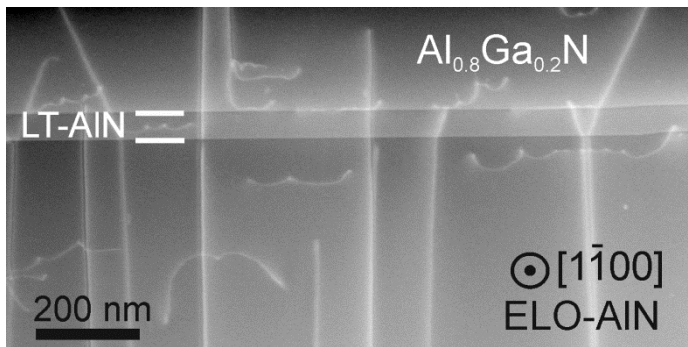


Fig. 4 Cross-sectional ADF-STEM image of the ELO AlN/LT-AlN/ $\text{Al}_{0.8}\text{Ga}_{0.2}\text{N}$ interface region

As visible, TD line inclination starts already at the ELO AlN/LT-AlN interface. This observation suggests that a certain Ga incorporation into the LT-AlN layer might take place. It is known that at the growth temperature of 1250°C some residual Ga atoms from the reactor environment can be incorporated into the LT-AlN. Using energy dispersive X-ray spectroscopy we have proved parasitic Ga incorporation into LT-AlN resulting in an actual Al content x of about 0.9 in LT-AlN.

4. Conclusions

$\text{Al}_x\text{Ga}_{1-x}\text{N}$ layers with $x \geq 0.5$ can successfully be grown on ELO AlN/sapphire templates. The defect structure in the layers depends on the TDD of the ELO substrate and the Al content x . In the case of $x = 0.5$ additional dislocation creation is observed both at the LT-AlN/ $\text{Al}_{0.5}\text{Ga}_{0.5}\text{N}$ interface and at the Ga-rich facets formed at the surface steps of ELO AlN substrates. In the case of high Al content, i.e. $x = 0.8$, $\text{Al}_x\text{Ga}_{1-x}\text{N}$ layers can be grown with the same TDD as in the underlying ELO AlN, although a 30° bending of the TDs toward the $\langle 1-100 \rangle$ directions was observed at the ELO AlN/LT-AlN interface.

Acknowledgement

This work has been partially supported by the German Federal Ministry of Education and Research (BMBF) (03WKBT01C) and the German Research Foundation (DFG) within the Collaborative Research Center 787.

References

- [1] Jiang H, Egawa T, Hao M, and Liu Y, 2005 *Appl. Phys. Lett.* **87** 241911
- [2] Imura M, Nakano K, Fujimoto N, Okada N, Balakrishnan K, Iwaya M, Kamiyama S, Amano H, Akasaki I, Noro T, Takagi T, and Bandoh A, 2006 *Jpn. J. Appl. Phys.* **45** 8639-8643
- [3] Iida K, Kawashima T, Iwaya M, Kamiyama S, Amano H, Akasaki I, and Bandoh A, 2007 *J. Cryst. Growth* **298** 265 – 267
- [4] Zeimer U, Kueller V, Knauer A, Mogilatenko A, Weyers M, and Kneissl M, 2013 *J. Cryst. Growth* **377** 32-36
- [5] Jain R, Sun W, Yang J, Shatalov M, Hu X, Sattu A, Lunev A, Deng J, Shturm I, Bilenko Y, Gaska R, and Shur M S, 2008 *Appl. Phys. Lett.* **93** 051113
- [6] Kueller V, Knauer A, Zeimer U, Rodriguez H, Mogilatenko A, Kneissl M, and Weyers M, 2011 *phys. stat. sol. (c)* **8** 2022-2024
- [7] Follstaedt D M, Lee S R, Allerman A A, Floro J A, 2009 *J. Appl. Phys.* **105** 083507